5.2 *Strength*

The mechanical strength of a brittle material such as alumina depends on fl (cracks) in the alumina surface. When a tensile stress is applied perpendicular t deep, thin crack, the stress at the tip of the crack is greatly magnified above applied stress. Thus, the surface condition of a brittle solid determines it streng Surface flaws develop from abrasion, so the higher the abrasion resistance of a bri solid the greater its practical strength. Strengths of alumina are given in Table 7.

If a solid has no surface or internal flaws (a "perfect" lattice), it should have v high strength. Various theoretical equations for this ultimate strength S of a bri solid have been proposed; one is [16]

$$S^2 = E\gamma/4b \qquad (4$$

in which E is Young's modulus, γ is the surface energy, and b the lattice parame With $E = 403$ GPa (Table 4), $\gamma = 6.0$ J m^{-2} [17, 18], and $b = 0.177$ nm, the ultim strength S of alumina is about 58 GPa. This value is very high because of the hi bond strength of alumina; for example, silicate glasses and quartz have theoreti strength values of 18 GPa or lower.

Practical strengths of brittle materials vary over wide ranges depending on th surface condition and history. For alumina, tensile or bonding strengths vary ove wide range of values because of different surface conditions, resulting in differ flaw depths and flaw distributions. See [19] for a discussion of flaw distributi functions. The strength values for alumina are higher than for most other oxides; course all of these strengths are far smaller than the theoretical strength, and depe strongly on the history and treatment of the samples. As the temperature increas the strength of alumina decreases (as shown in Table 7) because of the increase atomic vibrations and reduction in bond strength, just as for the reduction in elas modulus with temperature. The strength of polycrystalline alumina depends strong on its grain size, as shown by one set of strength values from [2]. See also [20] f strengths of alumina machined and annealed at different temperatures. The streng also decreases as the alumina becomes more porous, as shown in Table 8; isolat pores increase the applied stress on their surfaces, and open porosity means mu more surface for flaw development.

Table 7 Bend strengths of alumina in MPa

Theoretical strength 58,000 at 25°C				Ref
Single crystals (sapphire) 300–700 at 25°C				
Polycrystals with simila				
as a function of grair				
Grain size →	1–2	10–15	40–50	2
Temp (°C)				
25°C	460	330	240	
400°C	360	260	230	
1,000°C	340	260	210	
1,350°C	260	110	97	

MASIMO 1054
Masimo v. Apple
IPR2023-00634

Table 8 Effect of porosity on the bend strength of polycrystalline alumina at 25°C from [2]

Porosity (%)	Strength (MPa)
0	269
10	172
20	110
30	76
40	55
50	47

5.3 *Fatigue*

The strengths of crystalline and glassy oxides decrease with time under a constant applied load. This static fatigue is usually modeled with a power law equation between times to failure t when a sample is subjected to an applied stress s:

$$\log t = c - n \log s \tag{5}$$

in which c is a constant and the stress exponent n is a measure of the susceptibility of the material to fatigue. The larger the n value the more resistant the material is to fatigue. Typical values of n for silicate glasses are 13 or lower [21]; for alumina an n value of about 35 was found [21], showing that alumina has much better fatigue resistance than most other oxides under ambient conditions.

This fatigue in oxides results from reaction with water, which can break the cation–oxygen bonds in the material; for example in alumina:

$$\mathrm{Al - O - Al + H_2O = AlOH + HOAl} \tag{6}$$

Thus, when the ambient atmosphere is dry the fatigue failure time is long, and as the humidity increases the fatigue time decreases.

5.4 *Hardness*

The hardness of a material is measured by pressing a rod tip into a material and finding the amount of deformation from the dimensions of the resulting indentation. Hardness measu but hard to interpret. The stress distribution ing, elastic and anelastic deformation, faulting, and plastic deformation are all possible around the indentation. Alumina is one of the hardest oxides. On the nonlinear Mohs scale of one to ten, alumina is nine and diamond is ten, but diamond is about a factor of three harder than alumina. Some approximate Knoop hardness (elongated pyramidal diamond indenter) values for alumina are given as a function of temperature in Table 9, and in Table 10 for some hard ceramics [22, 23]. It is curious that the hardness of alumina decreases much more than the strength as the temperature is increased.

MASIMO 1054
Masimo v. Apple
IPR2023-00634

Table 9 Knoop hardness of alumina as a function of temperature

T (K)	Hardness (kg mm^{-2})
400	1,950
600	1,510
800	1,120
1,000	680
1,200	430
1,400	260
1,600	160

Table 10 Knoop hardness values of some ceramics at 25°C from [2, 22]

Material	Hardness (kg mm^{-2})
Diamond	8,500
Alumina	3,000
Boron carbide	2,760
Silicon carbide	2,480
Topaz ($Al_{12}Si_6F_{10}O_{25}$)	1,340
Quartz (SiO_2)	820

5.5 *Creep*

Creep is the high-temperature deformation of a material as a function of time. Oth high-temperature properties related to creep are stress and modulus relaxation, inte nal friction, and grain boundary relaxation. The creep rate increases strongly wit temperature, and is often proportional to the applied stress. Microstructure (grai size and porosity) influences the creep rate; other influences are lattice defect stoichiometry, and environment. Thus, creep rates are strongly dependent on sampl history and the specific experimental method used to measure them, so the onl meaningful quantitative comparison of creep rates can be made for samples with th same histories and measurement method. Some torsional creep rates of differer oxides are given in Table 11 to show the wide variability of creep values. Compare with some other high temperature materials such as mullite ($3Al_2O_3 \cdot 2SiO_2$), alumin has a higher creep rate, which sometimes limits its application at high temperature (above about 1,500°C). See [24] for a review of creep in ceramics and [25] for review of creep in ceramic–matrix composites.

5.6 *Plastic Deformation*

At high temperatures (above about 1,200°C) alumina can deform by dislocatio motion. The important paper by Merritt Kronberg [26], see also [1], p. 32, an [27], showed the details of dislocation motion in alumina. Basal slip on the close packed oxygen planes is most common in alumina, with additional slip system on prism planes.

MASIMO 1054
Masimo v. Apple
IPR2023-00634

Table 11 Torsional creep rates of some polycrystalline oxides at 1,300°C and 124 MPa applied stress (from [23], p. 755)

Material	Creep rate ($\times 10^5 h^{-1}$)
Al_2O_3	0.13
BeO	30
MgO (slip cast)	33
MgO (pressed)	3.3
$MgAl_2O_4$, spinel (2–5 μm grains)	26
$MgAl_2O_4$ (1–3 μm grains)	0.1
ThO_2	100
ZrO_2	3

5.7 *Fracture Toughness*

The fracture toughness K_{IC} of a brittle material is defined as

$$K_{IC} = YS\sqrt{c} \tag{7}$$

in which S is the applied stress required to propagate a crack of depth c, and Y is a geometrical parameter. Values of K_{IC} are often measured for ceramics from the lengths of cracks around a hardness indent. K_{IC} is not material parameter; it depends on sample history and many uncontrolled factors. It is based on the Griffith equation, which gives a necessary but not sufficient criterion for crack propagation [18]. Thus K_{IC} is not a very useful quantity for defining mechanical properties of brittle material. A value of about 3.0 $MPam^{1/2}$ is often found for alumina [1].

6 Thermal and Thermodynamic Properties

6.1 *Density and Thermal Expansion*

The density of alpha alumina at 25°C is 3.96 g cm^{-3}, which gives a specific volume of 25.8 $cm^3 mol^{-1}$ or 0.0438 nm^3 per Al_2O_3 molecule. Densities of other aluminas are given in Table 12.

The coefficient of thermal expansion α of alumina at different temperatures is given in Table 13. Often an average value of α is given over a range of temperatures, but the slope of a length vs. temperature plot at different temperatures is a more accurate way of desc

6.2 *Heat Capacity (Specific Heat) and Thermodynamic Quantities*

The specific heat, entropy, heat and Gibbs free energies of formation of alumina are given in Table 14, from [28]. Above 2,790°K, the boiling point of aluminum, there is a discontinuous change in the heat of formation of alumina.

MASIMO 1054
Masimo v. Apple
IPR2023-00634

Table 12 Densities of anhydrous and hydrated aluminas

Material	Density (g cm^{-2})
Sapphire (α-$A_{12}O_3$)	3.96
γ-Al_2O_3	3.2
δ-Al_2O_3	3.2
κ-Al_2O_3	3.3
θ-$A_{12}O_3$	3.56
$Al(OH)_3$ gibbsite	2.42
AlOOH diaspore	3.44
AlOOH boehmite	3.01

From [1]

Table 13 The coefficient of linear thermal expansion of α–alumina as a function of temperature

Temp. (°C)	$d\alpha/dT$ ($\times 10^6$ per °C)
1,000	12.0
800	11.6
600	11.1
400	10.4
200	9.1
100	7.7
50	6.5

From [23]

Table 14 Specific heat and thermodynamic properties of α-alumina as a function of temperature

	Specific heat	Entropy	Heat of formation	Free energy of formation
T (K)	J mol^{-1} K^{-1}		kJ mol^{-1}	
0	0	0	−1663.608	−1663.608
100	12.855	4.295	−1668.606	−1641.692
200	51.120	24.880	−1673.388	−1612.636
298.15	79.015	50.950	−1675.692	−1582.275
400	96.086	76.779	−1676.342	−1550.226
600	112.545	119.345	−1675.300	−1487.319
800	120.135	152.873	−1673.498	−1424.931
1,000	124.771	180.210	−1693.394	−1361.437
1,200	128.252	203.277	−1691.366	−1295.228
1,400	131.081	223.267	−1686.128	−1229.202
1,600	133.361	240.925	−1686.128	
1,800	135.143	256.740		
2,000	136.608	271.056		
2,200	138.030	284.143	−1676.485	−969.681
2,327	138.934	291.914	Melting temperature	
2,400	139.453	296.214	−1672.963	−905.582
2,600	140.959	307.435	−1669.279	−841.781
2,800	142.591	317.980	−2253.212	−776.335
3,000	144.474	327.841	−2244.729	−671.139

From [28]

MASIMO 1054
Masimo v. Apple
IPR2023-00634

6.3 Vaporization of Alumina

There is a detailed discussion of the vaporization behavior of alumina and other oxides in [29]. The main vapor species over alumina are Al, AlO, Al_2O, and AlO_2, depending on the temperature and oxidizing or reducing conditions in the surrounding atmosphere. Under reducing conditions Al and Al_2O are predominant; in 0.2 bar O_2, both AlO and AlO_2 are the main species [30].

Two examples of quantitative data of vapor pressure as a function of temperature are given in Table 15.

The boiling temperature of alumina at one atm pressure is about 3,530°C with a heat of vaporization of about 1,900 kJ mol^{-1} at 25°C [2], when compared with the melting temperature of 2,054°C, and a heat of fusion of about 109 kJ mol^{-1} at 25°C [31].

6.4 Thermal Conductivity

The thermal conductivity of α-alumina single crystals as a function of temperature is given in Table 16 (from [2, 23]). Heat is conducted through a nonmetallic solid by lattice vibrations or phonons. The mean free path of the phonons determines the thermal conductivity and depends on the temperature, phonon–phonon interactions, and scattering from lattice defects in the solid. At temperatures below the low temperature maximum (below about 40°K), the mean free path is mainly determined by the sample size because of phonon scattering from the sample surfaces. Above the maximum, the

Table 15 The pressure of AlO vapor and total vapor pressure in equilibrium with α-Al_2O_3 as a function of temperature, for reducing and neutral conditions

Temp. (K)	Log vapor pressure of AlO, *P* (bar) [29]
1,520	−15
1,630	−13
1,750	−11
1,900	−9
2,020	−7
2,290	−5
Temp. (K)	Log total vapor pressure, *P* (atm.) [2, 31]
	.06
	.99
	.78
2,393	−4.77
2,399	−4.66
2,459	−4.42
2,478	−4.24
2,487	−4.04
2,545	−3.70
2,565	−3.89
2,605	−3.72

MASIMO 1054
Masimo v. Apple
IPR2023-00634

Table 16 Thermal conductivity of single crystal α-Al_2O_3

Temp. (K)	Conductivity ($J\ s^{-1}\ mK^{-1}$)	Temp. (°C)	Conductivity ($J\ s^{-1}\ mK^{-1}$)
0	0	25	36
10	1,200	100	29
20	3,800	300	16
40	5,900	500	10
50	5,000	700	7.5
60	2,300	900	6.3
80	790	1,100	5.9
100	400	1,300	5.9
200	100	1,500	5.4
		1,700	5.9
		1,900	6.3

From [2, 23]

conductivity decays approximately exponentially because of phonon–phonon inte tions. At high temperatures (above about 800°C), the phonon mean free path is of order of a lattice distance, and becomes constant with temperature. There is a m more detailed discussion of phonon behavior in ceramics and glasses in [23, 32]. velocity v of a phonon or sound wave in a solid can be found from the formula

$$v^2 = E/\rho \qquad (1$$

in which E is Young's modulus and ρ is the density, so this velocity in alumin $10.1(10)^3$ m s^{-1} at 25°C. This result is close to the measured value of 10.845 m s^{-1}.

7 Electrical Properties

7.1 *Electrical Conductivity*

There have been a large number of studies of electrical conductivity of alumina, w widely different values being reported. Papers before 1961 are listed in [33] and thc from 1961 to 1992 in [34].

Anyone interested in the electrical conductivity of alumina should read carefu the papers of Will et al. [34]. These authors measured the electrical conductivity highly pure and dry sapphire from 400°C to 1,300°C; the elemental analysis of th sapphire samples is given in Table 17, and showed less than 35 ppm total impuritie Particularly significant is the low level of alkali meta provi ionic conduction in oxides.

The measurements in [34] were ıard ri configuration on disc samples, and in a vacuum of 10^{-7}–10^{-8} Torr. A nonsteady-sta voltage sweep technique was used for the measurements. The results are in Table 18 a Fig. 3 for conductivity along the x-axis. Between 700°C and 1,300°C, the activatic energy was about 460 kJ mol^{-1} (4.8 eV) and between 400 and 700°C it was 39 kJ mol (0.4 eV). The great care taken with these measurements and the high purity of t sapphire make them definitive for the electrical conductivity for pure, dry alumina.

MASIMO 1054
Masimo v. Apple
IPR2023-00634

Table 17 Chemical analysis of sapphire for electrical conductivity measurements, from [34]

Element	Conc. (ppm)	Element	Conc. (ppm)
Iron	8	Potassium	<5
Silicon	6	Sodium	<3
Calcium	3	Nickel	<3
Magnesium	0.6	Chromium	<3
Beryllium	0.1	Lithium	<2

Table 18 Electrical conductivity of pure, dry sapphire

Temp. (°C)	Log conductivity ($ohm^{-1} cm^{-1}$)
1,300	7.46
1,200	8.48
1,100	9.70
1,000	11.14
900	12.88
800	14.24
700	15.20
600	15.32
500	15.70
400	16.08

From [34]

After 650 h electrolysis at 1,200°C, the conductivity remained constant, showing it was electronic and nonionic [34]. The authors [34] interpreted their results in terms of electrical conductivity of a wide-band semiconductor. The high-temperature portion resulted from intrinsic conductivity with equal numbers of holes and electrons as carriers; twice the activation energy gives the band gap of about 920 kJ mol^{-1}, or 9.6 eV, which is close to the band gap of 8.8 eV calculated from the optical absorption edge in the ultra-violet spectral range (see Sect. 9.2 on optical absorption). The low activation energy portion at low temperatures was attributed to extrinsic electronic conductivity from ionization of impurities. The authors suggested that silicon as a donor atom was the most likely impurity resulting in the low temperature conductivity. The interpretation of extrinsic conduction in the low activation range agrees well with the results of several other studies of the electrical conductivity of alumina [35–38], which showed close to the same conductivity and activation energy at high temperatures, but a transition to the low activation energy regime at higher temperatures than 700°C, presumably because of more impurities in the samples in those studies.

The electrical conductivity of alumina parallel to the *c*-axis was found to be a factor of 3.3 higher than perpendicular to this axis [34].

Of special int ntal results for the conductivity at tempera- ing temperature of 2,054°C of alumina [39], which fall very close to an extrapolation of the data from [34] up to 1,300°C, with the same activation energy. Thus the intrinsic electrical conductivity σ in/ohm cm from 700°C to the melting point follows the equation:

$$\log \sigma = 7.92 - 24{,}200 / T \qquad (9)$$

where T is in Kelvin.

MASIMO 1054
Masimo v. Apple
IPR2023-00634

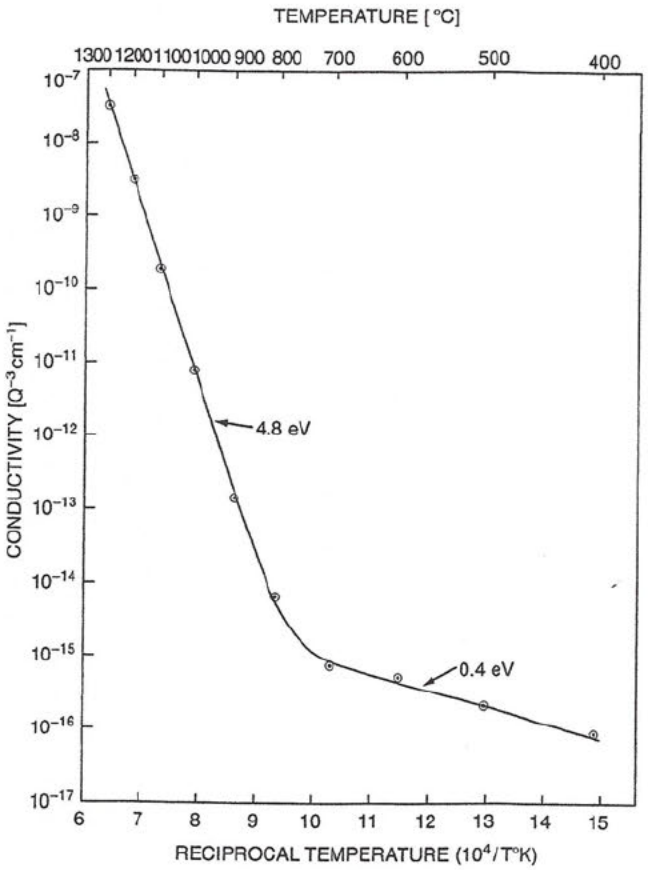


Fig. 3 The electrical conductivity of pure, dry sapphire along the *c*-axis. Points, measured values. From [34]

The electrolysis experiments of Ramirez et al. [40] show that when alumina contains some water (OH groups), the electrical conductivity results from the transport of hydrogen ions (actually hydronium ions, H_3O^+; see [41] for discussion).

The diffusion coefficient of H_3O^+ ions at 1,300°C calculated [41] from the experiments in [40] is $2.3(10)^{-9}\,cm^2s^{-1}$. This value is close to measured values of the diffusion coefficients of water in alumina [42]. Thus the mechanism of the diffusion of water in alumina is the transport of H_3O^+ ions, and these cal conductivity when the water concentration is high enough.

To calculate the minimum concentrat ıte to the electrical conductivity, one can use the Einstein equation:

$$C = RT\sigma / Z^2F^2D \qquad (10)$$

in which R is the gas constant, Z the ionic charge (valence), F the Faraday, and D the diffusion coefficient. The electrical conductivity at 1,300°C from [34] was 2.29

MASIMO 1054
Masimo v. Apple
IPR2023-00634

$\times 10^{-11}$/ohm cm. Thus with $D = 2.29(10)^{-9}$ cm^2 s^{-1}, a concentration of $1.13(10)^{-8}$ mol cm^{-3} of carriers results if one assumes that the conductivity in the samples in [34] results from H_3O^+ transport (which, of course, it does not); this concentration is $1.45(10)^{-7}$ carriers per Al atom in alumina. The concentration of H^+ in the alumina samples of [40] can be calculated from their highly sensitive infrared absorption measurements to be about $4.7(10)^{-7}$ per Al atom. Thus one can conclude that for H_3O^+ concentrations above about 10^{-8} mol cm^{-3} (3×10^{-7} ions per Al atom), there will be a contribution of these ions to the conductivity, whereas for lower H_3O^+ concentrations the conductivity will be mainly electronic.

The activation energy for water diffusion in alumina is about 220 kJ mol^{-1} (2.3 eV) from [42], so that many of the earlier results on electrical conductivity of alumina, for example, those summarized in [33], probably result from water transport at lower temperature; at higher temperatures, electronic conductivity will predominate, because of the high activation energy of intrinsic electronic conductivity. If the alumina is "dry" (H_3O^+ concentration below 10^{-8} mol cm^{-3}) low activation energy extrinsic electronic conduction will be dominant at lower temperatures, resulting from donor and receptor impurities in the alumina.

7.2 *Dielectric Properties*

The dielectric constant of alumina is given in Table 19 as a function of temperature and crystal orientation. The dielectric constant increases slightly up to 500°C, and is quite dependent on orientation. Very low dielectric loss values for sapphire have been reported [2], but are questionable. With reasonable purity, loss tangents below 0.001 are likely. Actual values probably depend strongly on crystal purity.

7.3 *Magnetic Properties*

Alumina is diamagnetic with a susceptibility less than 10^{-6} [2].

8 Diffusion in Alumina

Experimental volume diffusion coefficients of substances in alumina are summarized in ref. 41. Values for the parameters D_0 and Q (activation energy) from the Arrhenius equation:

$$D = D_0 \exp(-Q / RT) \tag{11}$$

ant of sapphire as a function of frequencies from 10^3 to 10^9 Hz (from [2]). Orientation to c axis

Temp. (°C)	I	II
25	9.3	11.5
300	9.6	12.1
500	9.9	12.5

MASIMO 1054
Masimo v. Apple
IPR2023-00634

The fastest diffusing substance in alumina is hydrogen (H_2). Fast-diffusing cation sodium, copper, silver, with hydroniums (H_3O^+) the fastest of these monovalent ons. Many other di- and trivalent cations have diffusion coefficients interme between these fast-diffusing ions and the slowest diffusers, the lattice elements al num and oxygen, which have about the same diffusion coefficients.

A number of experimenters have calculated diffusion coefficients D from "tail diffusion profiles in alumina, and attributed these D values to diffusion along dislocat subboundaries, or grain boundaries. However, this attribution is doubtful in most c as discussed in [41]. In only two studies [43, 44] is it likely true diffusion along g boundaries or dislocations was measured [41]. Mechanisms of diffusion in alu are uncertain; a variety of charged defects have been suggested to control diffusic alumina, but no interpretation is widely accepted because of discrepancies experimental results. I have suggested that oxygen and aluminum diffusion in alur results from transport of aluminum monoxide (AlO), and that AlO defects in alumina structure are important in diffusion. These speculations have some support, need more work to confirm them.

9 Chemical Properties

The decomposition of alumina at high temperatures can be deduced from its va pressure; see Sect. 6.3 and Table 15.

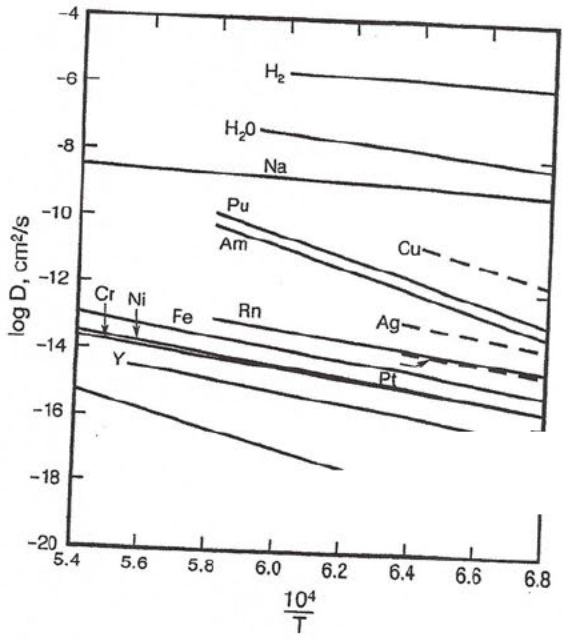


Fig. 4 Log diffusion coefficients vs. $10^4/T$ for selected substances diffusing in alumina. From [41

MASIMO 1054
Masimo v. Apple
IPR2023-00634

9.1 Reactions with Metals

The chemical reactions of alumina with other substances can best be explored from the thermodynamic properties of these reactions. If the Gibbs free energy ΔG of the reaction at a particular temperature is negative, the reaction tends to take place, and if ΔG this energy is positive the reaction tends not to occur. These considerations are modified by concentrations (more properly, thermodynamic activities) of the components as expressed in an equilibrium constant of the reaction. See books on thermodynamics for more details, for example [45].

The relative Gibbs free energies of the reactions of metals with oxygen tell whether or not a particular metal will displace the aluminum in alumina. The reaction of aluminum with oxygen is

$$\frac{4}{3}Al + O_2 = \frac{2}{3}Al_2O_3 \qquad (12)$$

All of the oxidation reactions with metals are written with one mole of O_2 reacting for consistent comparison. This is the format for reactions plotted in an Ellingham diagram (see [46]). The Gibbs free energies of some of these oxidation reactions are given in Table 20, taken from [28, 29, 46–48]. If the Gibbs free energy of the reaction is higher than that of aluminum ($-845.6\,kJ\ mol^{-1}$ for reaction (12)), then this metal will react with alumina, displacing all the aluminum in any alumina in contact with the metal, either solid, liquid, or vapor. For example for yttrium:

$$\frac{4}{3}Y + O_2 = \frac{2}{3}Y_2O_3 \qquad (13)$$

the Gibbs free energy is $-1017\,kJ\ mol^{-1}$, so yttrium will displace aluminum from alumina:

$$2Y + Al_2O_3 = 2Al + Y_2O_3 \qquad (14)$$

The free energy change of reaction 14 can be deduced from the values for Eqs. (12) and (13) from Table 20 to be $-256\,kJ\ mol^{-1}$, showing the tendency for yttrium to displace aluminum. If the free energy shown in Table 20 is less than that for oxidation of aluminum, the metal will not react with alumina. Thus at 1,000°C, sodium and potassium vapors (1 atm) do not react with alumina, but 1 atm. of lithium vapor does. Liquid alkaline earths metals such as Mg, Ca, Sr, and Ba react with alumina at 1,000°C and displace aluminum metal. The relative tendency of reactions of solid and liquid metals with alumina does not change much with temperature. Of course at low temperatures (below about 500°C), the rates of reactions can be slow, even if the thermodynamics show a tendency to react. Gibbs free energies for other temperatures can be calculated from data in the therm 29, 46–48].

9.2 Reactions with Nonmetals

The halides Cl_2, Br_2, and I_2 do not react with alumina, but fluorine (F_2) does:

$$2Al_2O_3 + 6F_2 = 4AlF_3 + 3O_2 \qquad (15)$$

MASIMO 1054
Masimo v. Apple
IPR2023-00634

Table 20 Gibbs Free energies of reactions of metals with 1 atm. of oxygen at 1,000°C from [28, 29, 46–48]

Solid metals	$-\Delta G$ (kJ mol^{-1})	Liquid metals	$-\Delta G$
Y	1,017		
Zr	849	Ca	1,013
Ti	678	CE	962
Si	644	Mg	937
V	619	Ba	879
Mn	586	Li	870
Cr	544	Al	845.6
One atm. of metal vapor	$-\Delta G$ (kJ/mol)		
Na	444		
Zn	418		
K	326		

Metal + O_2 = oxide

At 1,000°C the Gibbs free energy for this reaction is about −2133 kJ mol^{-1}, showing a strong tendency to react.

Reactions of the gases H_2, H_2O, CO, and CO_2 with alumina can be deduced from the reactions:

$$Al_2O_3 + 3H_2 = 2Al + 3H_2O \quad (16)$$

$$Al_2O_3 + 3CO = 2Al + 3CO_2 \quad (17)$$

At equilibrium at 1,000°C the ratio of H_2/H_2O is about 10^{10} and CO/CO_2 about $2(10)^{10}$. It is impossible to reduce the water or carbon dioxide levels so low in any practical reaction process, so effectively H_2 and CO do not reduce Al_2O_3. Even at 2,000°C these ratios are about $3(10)^4$ and $2(10)^5$, which are difficult levels to maintain in practice. A possible reaction of alumina with carbon is

$$2Al_2O_3 + 6C = Al_4C_3 + 3CO_2 \quad (18)$$

However, the Gibbs free energy of this reaction is +1131 kJ mol^{-1} at 1,000°C and +504.6 kJ mol^{-1} at 2,000°C, so it will take place only at very low carbon dioxide concentrations.

Other chemical reactions of alumina can be examined with the thermodynamic data in [28–30, 47–48].

9.3 *Reactions of Alumina in Aq*

Alumina is amphoteric, which means that it dissolves in acidic and basic solutions, but not in neutral aqueous solutions. The solubility of alumina in solutions of pH from about 4–9 is low; at 25°C it is less than 10^{-7} mol l^{-1} at pH 6 [1]. Alternatively, alumina dissolves readily in strong acids (HCl, HNO_3, H_2SO_4) and strong bases (NaOH, KOH) at temperatures well above ambient (e.g., 90°C).

MASIMO 1054
Masimo v. Apple
IPR2023-00634

10 Optical Properties

10.1 Refractive Index

The optical properties of solids can be studied with the complex refractive index n^*:

$$n^* = n + ik \tag{19}$$

in which n is the real part of the refractive index and k is the imaginary part or absorption index. Values of n and k from 0.008731 µm to 600 µm (142.000–0.00207 eV) are given to high accuracy and many wavelengths for alumina in [49]. In the wavelength range from 0.1454 µm to 4.000 µm (8.529–0.31 eV), the value of k for highly pure alumina is less than 10^{-6} [49, 50], so the alumina is effectively transparent. Values of n for this wavelength range are given to four significant figures in Table 21. Values of n in the fifth or sixth significant figure are different for different investigations, probably because of different purities of samples and different measuring techniques and errors. A two-term equation for n (ordinary ray) in this wavelength range is [2]

$$n = 1.74453 + \frac{0.0101}{\lambda - 0.1598} \tag{20}$$

with λ the wavelength in micrometers. This equation gives n accurately to about four significant figures (Table 21). A more accurate three-term Sellmeier equation is

$$n^2 - 1 = \frac{A_1 \lambda^2}{\lambda^2 - \lambda_1^2} + \frac{A_2 \lambda^2}{\lambda^2 - \lambda_2^2} + \frac{A_3 \lambda^2}{\lambda^2 - \lambda_3^2} \tag{21}$$

with the constants A_i and λ_i given in Table 22.

10.2 Optical Absorption

The absorption limit of 8.73 eV in Table 23 is close to the band gap of 8.8 eV for alumina. At energies lower than 8.73 eV, trace impurities and defects in the alumina lead to absorption tails as described in [49]. Values of n and k at higher energies than 8.73 eV are given in Table 23 to three or four significant figures. Values from different research groups can vary substantially [49]; those in Table 23 are from [50]. See [49] for n and k values at many more energies (wavelengths).

The values of [redacted] timum at about 13 eV, which can be attributed [redacted] tic processes in the ultra-violet spectral range [redacted]

Appreciable absorption begins in the infrared spectral range above a wavelength of 4.0 µm, as shown in Table 24; there are absorption peaks at 17.24 µm (580 cm^{-1}) and 22.73 µm (440 cm^{-1}), which result from lattice vibrations. For more details see [49].

The optical anisotropy of alumina results in slightly different n and k values for the ordinary and extraordinary ray, as shown in detail in [49] (see Table 22). This anisotropy is related to the hexagonal (rhombohedral) structure of the alumina.

MASIMO 1054
Masimo v. Apple
IPR2023-00634

Table 21 Refractive Index of sapphire at 25°C in the spectral range where $k < 10^{-6}$, from

Wavelength, λ, (μm)	Refractive index, n	Wavelength, λ (μm)	Refractive
0.1464	2.231	1.367	1.749
0.1603	2.070	1.530	1.747
0.1802	1.947	1.709	1.743
0.200	1.913	1.960	1.738
0.220	1.878	2.153	1.734
0.240	1.854	2.325	1.731
0.260	1.838	3.244	1.704
0.280	1.824	3.507	1.695
0.300	1.815	3.707	1.687
0.330	1.804	4.000	1.675
0.361	1.794		
0.405	1.786		
0.436	1.781		
0.486	1.775		
0.546	1.771		
0.579	1.769		
0.644	1.765		
0.707	1.763		
0.852	1.759		
0.894	1.758		
1.014	1.755		

Table 22 Refractive index [16], constants at 20°C from 0.2 to 5.5 mm, from [49, 50]

Term	Ordinary ray	Extraordinary ray
λ_1	0.0726631	0.0740298
λ_2	0.1193242	0.1216529
λ_3	18.028251	20.072248
A_1	1.4313493	1.5039759
A_2	0.65054713	0.5506141
A_3	5.3414021	6.5927379

The refractive index of alumina increases slightly with increasing temperature the visible and near-visible spectral range. The value of the temperature coefficien dT of the refractive index from wavelengths 0.4–0.8 μm is about $13(10)^{-6}°K^{-1}$ [49

10.3 Color of Alumina

Without impurities alumina is colorless. However, addition of transition metal ion alumina leads to spectacular colors, gem stones, ns such ruby lasers. Many aspects of color are discussed i

With the addition of about 1 out of hundred of the aluminum ions with chromium ions), alumina acquires a beautiful color and is known as ruby, one of the most prized gem stones. The red color res from transitions of electrons between energy levels in the ruby, as described in [5 p. 8Iff. Ruby also shows a bright red fluorescence when it is illuminated with ul violet light (energy of 4–5 eV). Ruby also shows pleochoism (multicolors); in pol ized light the color changes as the ruby crystal is rotated [51].

MASIMO 1054
Masimo v. Apple
IPR2023-00634

Table 23 Refractive index, n, and absorption index, k, of the ordinary ray for sapphire in the ultra-violet spectral range, at 25°C, from [49, 50]

Energy (eV)	Wavelength, λ, (μm)	n	k
142.000	0.008731	0.975	0.0130
120.000	0.010330	0.972	0.0177
100.206	0.01237	0.892	0.088
79.996	0.01550	0.929	0.130
60.001	0.02066	0.911	0.136
42.000	0.02952	0.859	0.098
30	0.04133	0.841	0.367
27.013	0.04590	0.605	0.317
24.113	0.05142	0.524	0.542
19.992	0.06202	0.800	0.983
18.008	0.06885	1.028	1.093
15.475	0.08012	1.142	1.125
13.582	0.09129	1.375	1.434
12.972	0.09558	2.581	1.573
12.361	0.1003	1.981	1.476
11.263	0.1101	2.400	1.131
10.292	0.1205	2.441	0.831
9.523	0.1302	2.559	0.686
8.852	0.1401	2.912	0.125
8.791	0.1410	2.841	0.037
8.760	0.1415	2.797	0.011
8.730	0.1420	2.753	0

Table 24 Refractive index, n, and absorption index, k, of the ordinary ray for sapphire in the infrared spectral range, at 25°C, from [49]

Wavelength, λ, (μm)	n	k
4.000	1.675	$1.30\ (10)^{-6}$
5.000	1.624	$3.76\ (10)^{-5}$
7.143	1.459	$3.60\ (10)^{-3}$
10.00	0.88	0.053
10.99	0.27	0.224
12.05	0.08	1.04
12.99	0.07	1.57
14.93	0.10	2.96
16.13	0.47	3.56
16.95	0.75	6.30
17.24	1.69	11.28
17.86	9.10	1.53
19.23	3.82	0.115
20.00	2.64	0.106
22.73	10.08	14.01
25.00	4.64	0.156
30.30	3.95	0.0145
33.33	3.69	0.00668
	3.26	0.0117
	3.19	0.0130
82.71	3.13	0.0085
100.0	3.12	0.0070
200.0	3.08	0.0035
333.3	3.07	0.0027
600.0	3.05	0.0015

MASIMO 1054
Masimo v. Apple
IPR2023-00634

The deep blue color or sapphire gems results from the addition of a few hundredths of one percent of iron and titanium impurities to alumina. The Fe^{2+} and Ti^{4+} ions substitute for aluminum in the sapphire, and when light of energy of 2.11 eV is shone on the sapphire, it is absorbed by the charge transfer reaction:

$$Fe^{2+} + Ti^{4+} = Fe^{3+} + Ti^{3+} \quad (22)$$

See [51], p. 140ff for a complete description of this process.

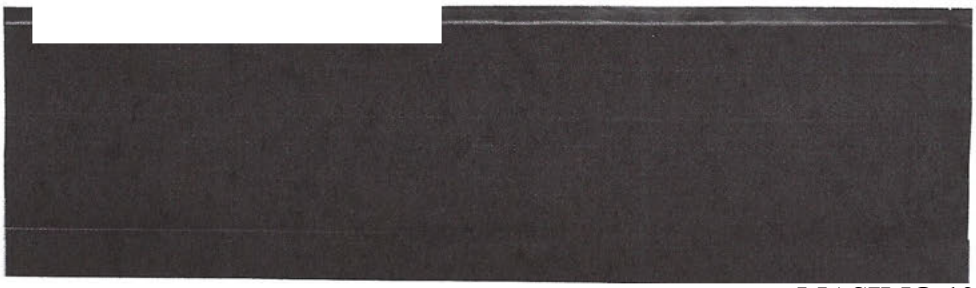
A variety of other colors are found in natural and synthetic alumina crystals [2, 51]. For example, an orange-brown color is produced by Cr^{4+} (padparadscha sapphire) [51]; different transition metal ions in different concentrations and oxidation states produce many colors.

11 Conclusion and Future Uses of Alumina

The properties of alumina listed in Sects. 4–10 show the unusual performance of pure alumina, leading to the variety of applications given in Table 1. Practical aluminas with impurities and defects have somewhat degraded properties, but often are superior to many other materials, and have a variety of specialized applications such as refractories, electronic components, and catalyst substrates. In [1] there are articles discussing the future of alumina. There will continue to be incremental improvements in processing methods and properties, leading to expansion of present applications. What really new areas of application of alumina are likely? These predictions are speculative, but the most promising new applications of alumina will probably be in electronic circuits, optical components, and biomaterials. Alumina fibers for composites and optics are attractive if they can be made pure, defect-free, and cheap. Because of its excellent properties other unsuspected applications of alumina will undoubtedly be developed.

Reference

1. L.D. Hart (ed.), *Alumina Chemicals*, The American Ceramic Society, Westerville, OH, 1990.
2. W.H. Gitzen, *Alumina as a Ceramic Material*, The American Ceramic Society, Westerville, OH, 1970.
3. Emphasizes defects and interfaces, especially grain boundaries, in alumina, *J. Am. Ceram. Soc.* **77**, [2] (1994).
4. Emphasizes grain boundaries, grain growth, and diffusion in alumina, *J. Am. Ceram. Soc.* **86** [4] (2003).
5. P. Richet, J.A. Xu, and H.K. Mao, Quasi-hydrostatic compression of ruby to 500 kbar, Phys. Chem. Min. **16**, 207–211 (1988).
6. A.P. Jephcoat, R.J. Hemley, H.K. Mao, and K.A. Goettel, X-ray diffraction of ruby (Al_2O_3: Cr^{3+}) to 175 GPa, *Physica B* **150**, 115–121 (1988).
7. K.T. Thomson, R.M. Wentzcovitch, and M.S.T. Bukowinski, Polymorphs of alumina predicted by first principles, *Science* **274**, 1880–1882 (1996).
8. A.H. Carim, G.S. Rohrer, N.R. Dando, S.Y. Tzeng, C.L. Rohrer, and A.J. Perrotta, Conversion of diaspore to corundum, *J. Am. Ceram. Soc.* **80**, 2677–80 (1997).
9. R.L. Coble, Transparent Alumina and Method of Preparation, U.S. Patent 3,026,210, March 20 (1967).



MASIMO 1054
Masimo v. Apple
IPR2023-00634

10. F.J. Klug, S. Prochazka, and R.H. Doremus, Alumina-silica phase diagram in the mullite region, *J. Am. Ceram. Soc.* **70**, 750–759 (1987).
11. E.N. Bunting, Phase equilibrium in the system Cr3O3–Al2O3, *Bur. Stand. J. Res.* **6**, 947–949 (1931).
12. E.M. Levin, C.R. Robbins, and H.F. *McMurdie, Phase Diagrams for Ceramists*, Vol. I–XIII, The American Ceramic Society, 1964–2002.
13. D.M. Roy and R.E. Barks, Subsolidus phase equilibrium in Al2O3–Cr2O3, *Nature*, **235**, 118–119 (1972).
14. C. Greskovich and J.A. Brewer, Solubility of magnesia in polycrystalline alumina at high temperatures, *J. Am. Ceram. Soc.* **84**, 420–425 (2001).
15. J.H. Gieske and G.R. Barsch, Pressure dependence of the elastic constants of single crystalline aluminum oxide, *Phys. Status Solidi* **29**, 121–131 (1967).
16. A. Kelly, *Strong Solids*, Chap. 1, Oxford University Press, London, 1973.
17. S.M. Wiederhorn in Mechanical and Thermal Properties of Ceramics, J.B. Wachtman, (ed.), NBS Special Publications 303, U.S. GPO, Washington, D.C., 1969, p. 217.
18. R.H. Doremus, Cracks and energy-criteria for brittle fracture, *J. Appl. Phys.* **47**, 1833–1836 (1976).
19. R.H. Doremus, Fracture statistics: A comparison of the normal, Weibull and type I extreme value distributions, *J. Appl. Phys.* **54**, 193–201 (1983).
20. S.C. Carniglia, Reexamination of experimental strength – vs. – grain – size data for ceramics, *J. Am. Ceram. Soc.* **55**, 243 (1972).
21. J.E. Burke, R.H. Doremus, W.B. Hillig, and A.M. Turkalo, Static Fatigue in Glasses and Alumina, in Materials Sci. Res. Vol. 5, W.W. Kriegel (ed.), Plenum Press, New York, 1971, pp. 435–444.
22. N.W. Thibault and H.Z. Nyquist, The measured Knoop hardness of hard substances and factors affecting its determination, *Trans. Am. Soc. Metals* **38**, 271–330 (1947).
23. W.D. Kingery, H.K. Bowen, and D.R. Uhlmann, *Introduction to Ceramics*, Wiley, New York (1976).
24. W.R. Cannon and T.G. Langdon, Creep of Ceramics, *J. Mater. Sci.* **18**, 1–50 (1983); **23**, 1–20 (1988).
25. A.H. Hynes and R.H. Doremus, Theories of creep in ceramics, *Crit. Rev. Solid State Mater. Sci.* **21**, 1–59 (1996).
26. M.L. Kronberg, Plastic deformation of single crystals of sapphire: Basal slip and twinning, *Aeta Met.* **5**, 507–529 (1957).
27. J.D. Snow and A.H. Heuer, Slip systems in Al2O3, *J. Am. Ceram. Soc.* **56**, 153–157 (1973).
28. M.W. Chase, NIST – JAVAF Thermochemical Tables, *J. Phys. Chem. Ref. Data, Monograph* **9**.
29. R.H. Tamoreaux, D.L. Hildenbrand and L. Brewer, High temperature vaporization behavior of oxides, *J. Phys. Chem. Ref. Data* **16**, 412 (1987).
30. L. Brewer and A.W. Searcy, Gaseous species of the Al–Al_2O_3 system, *J. Am. Chem. Soc.* **73**, 5308–5314 (1951).
31. R.V. Gains, H.C.W. Skinner, E.E. Foord, B. Mason, and A. Rosenzweig, *Dana's New Mineralogy*, Wiley, New York, 1977, p. 214.
32. E. Schreiber and O.L. Anderson, Pressure derivatives of the sound velocities of polycrystalline alumina, *J. Am. Ceram. Soc.* **49**, 184–190 (1966).
33. J. Pappis and W.D. Kingery, Electrical properties of single and polycrystalline alumina at high temperatures, *J. Am. Ceram. Soc.* **44**, 459 (1961).
34. F.G. Will, H.G. Lorenzi, and K.H. Janora, *J. Am. Ceram. Soc.* **75**, 295–304, 2790–2791 (1992).
35. O.T. Özkan and A.J. Moulson, The electrical conductivity of single crystal and polycrystalline aluminum oxide, *British J. Appl. Phys.* **3**, 983 (1970).
36. H.P.R. Frederike and W.R. Hosler, High temperature electrical conductivity of aluminum oxide, *Mater. Sci. Res.* **9**
37. K. Kituzawa and I :tion in single crystal and polycrystalline Al2O3 at (1979).
38. H.H. Kizilyali and P.R. Mason, DC and AC electrical conduction in single crystal alumina, *Phys. Status Solidi* **36**, 499 (1976).
39. E.E. Shpilrain, D.N. Kagan, L.S. Barkhatov, and L.I. Zhmakin, The electrical conductivity of alumina near the melting point, High Temperatures – High Pressures **8**, 177 (1976).
40. R. Ramirez, R. Gonzalez, J. Colera, and Y. Chen, Electric-field-enhanced diffusion of deuterons and protons in α-Al2O3 crystals, *Phys. Rev. B* **55**, 237–242 (1997).
41. R.H. Doremus, Diffusion in Alumina, *J. Appl. Phys.* **101**, 101301 (2006).

MASIMO 1054
Masimo v. Apple
IPR2023-00634

42. J.D. Fowler, D. Chandra, T.S. Elleman, A.W. Payne, and K. Verghese, Tritium diffusic and BeO, *J. Am. Ceram. Soc.* **60**, 55 (1977).
43. V.S. Stubican and J.W. Orenbach, Influence of anisotropy and doping on grain-bounda in oxide systems, *Solid State Ionics* **12**, 375 (1984).
44. X. Tang, and K.P.D. Lagerof, and A.H. Heuer, Determination of pipe diffusion coe undoped and magnesia doped sapphire (α-Al2O3); a study based on annihilation of dipoles, *J. Am. Ceram. Soc.* **86**, 560–565 (2003).
45. D.R. Gaskell, *Introduction to the Thermodynamics of Materials*, 4th edn.,Taylor a New York, 2003.
46. L.S. Darken and N.W. Gurry, *Physical Chemistry of Metals*, McGraw-Hill, New York
47. A. Paul, *Chemistry of Glasses*, Chapman and Hall, London, 1982, p. 157.
48. R.H. Doremus, *Diffusion of Reactive Molecules in Solids and Melts*, Wiley, New York 71, 191.
49. M.E. Thomas and W.J. Tropf in *Handbook of Optical Constants of Solids III*, I (ed.), Academic Press, New York, 1998, p. 653.
50. L.H. Malitson and M.J. Dodge, Refractive index and birefringence of synthetic sapphi *Soc. Am.* **62**, 1405 (1972).
51. K. Nassau, *The Physics and Chemistry of Color*, Wiley, New York, 1983.

MASIMO 1054
Masimo v. Apple
IPR2023-00634

EXHIBIT LLL

MASIMO 1054
Masimo v. Apple
IPR2023-00634

CERAMIC MATERIALS – PROGRESS IN MODERN CERAMICS

Edited by **Feng Shi**

INTECHOPEN.COM

MASIMO 1054
Masimo v. Apple
IPR2023-00634

Ceramic Materials – Progress in Modern Ceramics
Edited by Feng Shi

Published by InTech
Janeza Trdine 9, 51000 Rijeka, Croatia

Copyright © 2012 InTech
All chapters are Open Access distributed under the Creative Commons Attribution 3.0 license, which allows users to download, copy and build upon published articles even for commercial purposes, as long as the author and publisher are properly credited, which ensures maximum dissemination and a wider impact of our publications. After this work has been published by InTech, authors have the right to republish it, in whole or part, in any publication of which they are the author, and to make other personal use of the work. Any republication, referencing or personal use of the work must explicitly identify the original source.

As for readers, this license allows users to download, copy and build upon published chapters even for commercial purposes, as long as the author and publisher are properly credited, which ensures maximum dissemination and a wider impact of our publications.

Notice
Statements and opinions expressed in the chapters are these of the individual contributors and not necessarily those of the editors or publisher. No responsibility is accepted for the accuracy of information contained in the published chapters. The publisher assumes no responsibility for any damage or injury to persons or property arising out of the use of any materials, instructions, methods or ideas contained in the book.

Publishing Process Manager Ivona Lovric
Technical Editor Teodora Smiljanic
Cover Designer InTech Design Team

First published April, 2012
Printed in Croatia

A free online edition of this book is available at www.intechopen.com
Additional hard copies can be obtained from orders@intechopen.com

Ceramic Materials – Progress in Modern Ceramics, Edited by Feng Shi
p. cm.
ISBN 978-953-51-0476-6

MASIMO 1054
Masimo v. Apple
IPR2023-00634

Contents

Preface IX

Part 1 **Electronic Ceramics** 1

Chapter 1 **Characterization of PLZT Ceramics for Optical Sensor and Actuator Devices** 3
Ribal Georges Sabat

Chapter 2 **Electrode Size and Dimensional Ratio Effect on the Resonant Characteristics of Piezoelectric Ceramic Disk** 25
Lang Wu, Ming-Cheng Chure, Yeong-Chin Chen, King-Kung Wu and Bing-Huei Chen

Part 2 **Nano-Ceramics** 41

Chapter 3 **Fine Grained Alumina-Based Ceramics Produced Using Magnetic Pulsed Compaction** 43
V. V. Ivanov, A. S. Kaygorodov, V. R. Khrustov and S. N. Paranin

Chapter 4 **Advanced Sintering of Nano-Ceramic Materials** 65
Khalil Abdelrazek Khalil

Chapter 5 **Development of Zirconia Nanocomposite Ceramic Tool and Die Material Based on Tribological Design** 83
Chonghai Xu, Mingdong Yi, Jingjie Zhang, Bin Fang and Gaofeng Wei

Part 3 **Structural Ceramics** 107

Chapter 6 **Synthesis, Microstructure and Properties of High-Strength Porous Ceramics** 109
Changqing Hong, Xinghong Zhang, Jiecai Han, Songhe Meng and Shanyi Du

MASIMO 1054
Masimo v. Apple
IPR2023-00634

Chapter 7 **Composites Hydroxyapatite with Addition of Zirconium Phase 129**
Agata Dudek and Renata Wlodarczyk

Part 4 Simulation of Ceramics 149

Chapter 8 **Numerical Simulation of Fabrication for Ceramic Tool Materials 151**
Bin Fang, Chonghai Xu, Fang Yang, Jingjie Zhang and Mingdong Yi

Part 5 Ceramic Membranes 169

Chapter 9 **Synthesis and Characterization of a Novel Hydrophobic Membrane: Application for Seawater Desalination with Air Gap Membrane Distillation Process 171**
Sabeur Khemakhem and Raja Ben Amar

Chapter 10 **Fabrication, Structure and Properties of Nanostructured Ceramic Membranes 191**
Ian W. M. Brown, Jeremy P. Wu and Geoff Smith

MASIMO 1054
Masimo v. Apple
IPR2023-00634

Preface

As we all know, ceramic materials are inorganic, non-metallic, solid, and inert materials. Things are made from them by the action of heat and subsequent cooling, which may be crystalline or partly crystalline. The definition of ceramic is often restricted to inorganic crystalline materials, as opposed to the noncrystalline glasses, which involve several steps of the ceramic process, and their mechanical properties behave similarly to ceramic materials.

The history of ceramics is as old as civilization, and our use of ceramics is a measure of the technological progress of a civilization. Ceramics have important effects on human history and human civilization. Earlier transitional ceramics, several thousand years ago, were made by clay minerals such as kaolinite. Modern ceramics are classified as advanced and fine ceramics. Both include three distinct material categories: oxides such as alumina and zirconia, nonoxides such as carbide, boride, nitride, and silicide, as well as composite materials such as particulate reinforced and fiber reinforced combinations of oxides and nonoxides. These advanced ceramics, made by modern chemical compounds, can be used in the fields of mechanics, metallurgy, chemistry, medicine, optical, thermal, magnetic, electrical and electronics industries, because of the suitable chemical and physical properties. In particular, photoelectron and microelectronics devices, which are the basis of the modern information era, are fabricated by diferent kinds of optical and electronic ceramics. In other words, optical and electronic ceramics are the base materials of the modern information era.

Bulk ceramics are made into the desired shape by reaction in situ, or by "forming" powders into the desired shape, and then sintering to form a solid body. However, ceramic thin films can be made by chemical or physical deposition. Grains, secondary phases, grain boundaries, pores, micro-cracks, structural defects, and hardness microindentions consist of the microstructure of the ceramics, which are generally indicated by the fabrication method and process conditions.

To explain more about advanced ceramics, this book (organized by InTech – Open Access Publisher) has been written by different authors, who focus on modern ceramics. A feature of this text is that we keep in mind that many of today's high-tech ceramic materials and processing routes have their origin in the potter's craft, microstructures, and properties. Throughout the text we make connections to these

MASIMO 1054
Masimo v. Apple
IPR2023-00634

related fields. The text covers ceramic materials, from the fundamentals to industrial applications, including a consideration of safety and their impact on the modern technologies, including nano-ceramic, ceramic matrix composites, nanostructured ceramic membranes, porous ceramics, and sintering theory models of modern ceramics.

We thank all the authors and all the editors who contributed greatly to this book, and we hope that readers find it interesting.

Dr. Feng Shi
Shandong Normal University
China

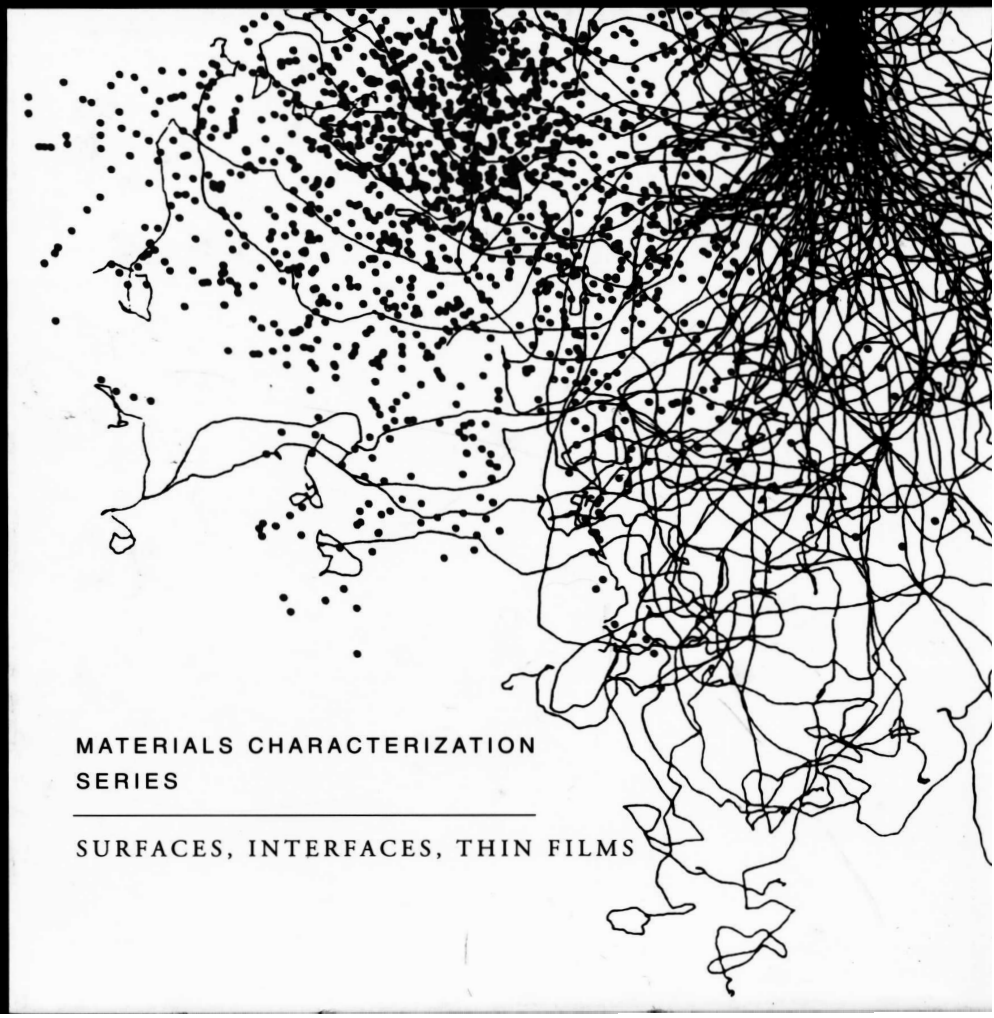
MASIMO 1054
Masimo v. Apple
IPR2023-00634

EXHIBIT MMM

MASIMO 1054
Masimo v. Apple
IPR2023-00634

CHARACTERIZATION OF CERAMICS

Ronald E. Loehman



MATERIALS CHARACTERIZATION SERIES

SURFACES, INTERFACES, THIN FILMS

MASIMO 1054
Masimo v. Apple
IPR2023-00634

CHARACTERIZATION OF CERAMICS

EDITOR

Ronald E. Loehman

MANAGING EDITOR

Lee E. Fitzpatrick

BUTTERWORTH-HEINEMANN
Boston London Oxford Singapore Sydney Toronto Wellington

MANNING
Greenwich

MASIMO 1054
Masimo v. Apple
IPR2023-00634

UNIVERSITY OF WISCONSIN - MADISON
LIBRARY

This book was acquired, developed, and produced by Manning Publications Co.
Designer: Christopher Simon
Editor: Deborah Oliver
Typesetter: Stephen Brill

Copyright © 1993 by Butterworth-Heinemann, a division of Reed Publishing (USA) Inc.

All rights reserved.

No part of this publication may be reproduced, stored in a retrieval system, or transmitted, in any form or by means electronic, mechanical, photocopying, or otherwise, without prior written permission of the publisher.

Recognizing the importance of preserving what has been written, it is the policy of Butterworth-Heinemann and of Manning to have the books they publish printed on acid-free paper, and we exert our best efforts to that end.

Library of Congress Cataloging–in–Publication Data
Characterization of ceramics/editor Ronald E. Loehman.
p. cm.—(Materials characterization series)
Includes bibliographical references and index.
ISBN 0-7506-9253-7
1. Ceramics. I. Loehman, Ronald E. II. Series.
TP807.C463 1992 92–21549
620.1'4 7dc20 CIP

Butterworth-Heinemann
80 Montvale Avenue
Stoneham, MA 02180

Manning Publications Co.
3 Lewis Street
Greenwich, CT 06830

1 0 9 8 7 6 5 4 3 2 1

Printed in the United States of America

MASIMO 1054
Masimo v. Apple
IPR2023-00634

engn TP 807 C463 1993 ARS7312

Contents

Preface to Series xi

Preface xii

Contributors xv

POWDER AND PRECURSOR PREPARATION BY SOLUTION TECHNIQUES

1.1 Introduction 1
Mixed Oxide Processing 2, Chemical Synthesis of Powders 2

1.2 Powder Characterization 3
Physical Characteristics 3, Chemical Properties 4

1.3 Precursor Powder Synthesis 8
Speciation and Supersaturation 8, Growth 10, Nucleation 19, Agglomeration 22

1.4 Summary 23

POWDER PREPARATION BY GAS-PHASE TECHNIQUES

2.1 Introduction 29

2.2 Powder Production by Thermal Decomposition Techniques 30
Aerosol Precursor Processes 30, Vapor Precursor Processes 33

2.3 Powder Production by Plasma Techniques 35

2.4 Powder Production by Supercritical Fluid Techniques 37

MASIMO 1054
Masimo v. Apple
IPR2023-00634

2.5 Powder Characterization 39

2.6 Summary 40

FORMATION OF CERAMIC FILMS AND COATINGS

3.1 Introduction 43

3.2 Film Deposition and Coating Processes 44
Physical Vapor Deposition 44, Chemical Vapor Deposition 45, Solution and Sol–Gel Techniques 45, Thermal Spray Processing 46, Hard Carbon Coatings 46

3.3 Physical Characterization 47
Density, Porosity and Voids 47, Morphology 48, Thickness 48, Surface Finish 49

3.4 Chemical Characterization 50
Elemental Analysis 50, Chemical State Analysis 53, Microstructure 56

3.5 Mechanical Characterization 57
Adhesion 57, Hardness 59, Internal Stress 60

3.6 Summary 60

CONSOLIDATION OF CERAMIC THICK FILMS

4.1 Introduction 63

4.2 Thick Film Processing 64

4.3 Characterization of Ceramic Thick Film Consolidation 65
Characterization of Films Before Thermal Processing 65, Characterization of Thick Films During Thermal Processing 68, Characterization of Sintered Thick Films 70

4.4 Summary 75

CONSOLIDATION OF BULK CERAMICS

5.1 Introduction 77

5.2 Ceramic Consolidation 78
Green Body Fabrication 78, Pre-Sinter Thermal Processing 79, Sintering/Thermal Consolidation 80

5.3 Characterization of Ceramics 82
Characteristics and Characterization of Green Ceramic Compacts 83, Characterization of Pre-Sinter Thermal Processes 90, Characteristics and Characterization of Sintered Ceramics 90

5.4 Summary 96

MASIMO 1054
Masimo v. Apple
IPR2023-00634

INORGANIC GLASSES AND GLASS-CERAMICS

6.1 Introduction 103

6.2 Possible Surface Analytical Artifacts 104

6.3 XPS Studies of Bonding in Glass 108

6.4 Corrosion in Water 110
Water Vapor 111, Aqueous Solutions 112

6.5 Glass Crystallization 114

CERAMIC MICROSTRUCTURES

7.1 Introduction 119

7.2 Bulk Microstructural Features 120
Grain Size, Shape, and Growth 120, Connectivity 122, Boundary Layers and Inclusions 123, Porosity and Density 123

7.3 Interfaces and Planar Defects 124
Grain Boundaries and Domain Boundaries 124, Heterogeneous Interfaces 125, Stacking Faults and Twins 126

7.4 Dislocations 127

7.5 Methods of Phase Identification 129
Phase Distribution 130, Crystal Structure of Phases 131, Chemical Composition of Phases 132

7.6 Stereology for Phase Quantification 133
Grain Size and Mean Lineal Intercept 134, Volume Fraction of Phases 135

7.7 Summary 135

CERAMIC REACTIONS AND PHASE BEHAVIOR

8.1 Introduction 137

8.2 Starting Materials 140

8.3 Phase Equilibria 140
General Aspects 140, Determining the Chemical and Structural Aspects 141, Determining the Physical Variables 154

8.4 Rates and Mechanisms of Reaction 156
General Considerations 156, Decomposition of Precursors 158, Solid–Solid Reactions 161, Solid–Liquid Reactions 164, Solid–Gas Reactions 165

8.5 Summary 166

MASIMO 1054
Masimo v. Apple
IPR2023-00634

MECHANICAL PROPERTIES AND FRACTURE

9.1 Introduction 169

9.2 The Fracture Process 169
Mechanical Strength of Brittle Materials 169, Flaws, Statistics of Fracture, and Measurement Techniques 171, Subcritical Crack Growth 173

9.3 Generation of Fracture Surface Features 174
Features Produced by Crack Interactions 174, Mist and Velocity Hackle 178

9.4 Procedures and Equipment Used in Fractography 181

9.5 Applications of Fractography 182
Failure Analysis Using Fractography 182, The Use of Fractography in Design Development 182, Fractography in Materials Development 186, Fractography in Materials Research 187

CERAMIC COMPOSITES

10.1 Introduction 189

10.2 Mechanical Properties of Ceramic Composites 191
R-Curve Behavior 191, Creep 193, Fracture Toughness 195, Flaws 198, Fatigue Crack Propagation Resistance 199, Fracture Mode 200, Adhesion 201

10.3 Oxidation Resistance of Ceramic Composites 202

10.4 Electrical Properties of Ceramic Composites 204
Piezoelectricity 204, Voltage-Dependent Conductivity 205

10.5 Summary 206

GLASS AND CERAMIC JOINTS

11.1 Introduction 211

11.2 Characterization of Interfaces 212

11.3 Methods of Joining 213
Mechanical Joining 213, Direct Joining 214, Indirect Joining 214

11.4 Fundamentals of Interfacial Bonding: Wetting and Spreading 216

11.5 Reactive Metal Brazing of Aluminum Nitride 219
Wetting Studies 219, Interfacial Reactions 222, XPS Characterization of Ti–AlN Interfaces 223, TEM Characterization of Ti–AlN Interfaces 224

11.6 Summary 225

MASIMO 1054
Masimo v. Apple
IPR2023-00634

ELECTRONIC AND MAGNETIC CERAMICS

12.1 Introduction 229

12.2 Insulators and Capacitor Materials 230
Ceramic Insulators 230, Ceramic Capacitor Materials 232

12.3 Piezoelectrics 234

12.4 Pyroelectric Ceramics 236

12.5 Ferroelectric Ceramics 237

12.6 Ceramic Superconductors 238

12.7 Ferrites 239

12.8 Ceramic Sensors 241

12.9 Ceramic Thin Films 242

NONDESTRUCTIVE EVALUATION

13.1 Introduction 253

13.2 X-ray Techniques 255
Radiography 255, Tomography 256

13.3 Ultrasonic Techniques 257
Background 257, Ultrasonic Time of Flight 258, Ultrasonic Spectroscopy 259, Scanning Laser Acoustic Microscopy (SLAM) 260, Acoustic Microscopy 260, Ultrasonic Birefringence 261

13.4 Other Techniques 261
Strain-Induced Optical Birefringence 261, Penetrant Techniques 261, Photoacoustic Microscopy 262, Infrared Microscopy 262, Acoustic Emission 262, Shearography 263, Lattice Distortion 263

13.5 Summary 264

APPENDIXES: TECHNIQUES SUMMARIES

1 Auger Electron Spectroscopy (AES) 269

2 Electron Energy-Loss Spectroscopy in the Transmission Electron Microscope (EELS) 270

3 Electron Probe X-Ray Microanalysis (EPMA) 271

4 Energy-Dispersive X-Ray Spectroscopy (EDS) 272

5 Fourier Transform Infrared Spectroscopy (FTIR) 273

6 Light Microscopy 274

7 Neutron Diffraction 275

MASIMO 1054
Masimo v. Apple
IPR2023-00634

8 Physical and Chemical Adsorption for the Measurement of Solid State Areas 276

9 Raman Spectroscopy 277

10 Rutherford Backscattering Spectrometry (RBS) 278

11 Scanning Electron Microscopy (SEM) 279

12 Scanning Transmission Electron Microscopy (STEM) 280

13 Scanning Tunneling Microscopy and Scanning Force Microscopy (STM and SFM) 281

14 Solid State Nuclear Magnetic Resonance (NMR) 282

15 Surface Roughness: Measurement, Formation by Sputtering, Impact on Depth Profiling 283

16 Transmission Electron Microscopy (TEM) 284

17 Variable-Angle Spectroscopic Ellipsometry (VASE) 285

18 X-Ray Diffraction (XRD) 286

19 X-Ray Fluorescence (XRF) 287

20 X-Ray Photoelectron Spectroscopy (XPS) 288

Index 289

MASIMO 1054
Masimo v. Apple
IPR2023-00634

This material may be protected by Copyright law (Title 17 U.S. Code)

Preface to Series

This Materials Characterization Series attempts to address the needs of the practical materials user, with an emphasis on the newer areas of surface, interface, and thin film microcharacterization. The Series is composed of the leading volume, *Encyclopedia of Materials Characterization*, and a set of about 10 subsequent volumes concentrating on characterization of individual materials classes.

In the *Encyclopedia*, 50 brief articles (each 10 to 18 pages in length) are presented in a standard format designed for ease of reader access, with straightforward technique descriptions and examples of their practical use. In addition to the articles, there are one-page summaries for every technique, introductory summaries to groupings of related techniques, a complete glossary of acronyms, and a tabular comparison of the major features of all 50 techniques.

The 10 volumes in the Series on characterization of particular materials classes include volumes on silicon processing, metals and alloys, catalytic materials, integrated circuit packaging, etc. Characterization is approached from the materials user's point of view. Thus, in general, the format is based on properties, processing steps, materials classification, etc., rather than on a technique. The emphasis of all volumes is on surfaces, interfaces, and thin films, but the emphasis varies depending on the relative importance of these areas for the materials class concerned. Appendixes in each volume reproduce the relevant one-page summaries from the *Encyclopedia* and provide longer summaries for any techniques referred to that are not covered in the *Encyclopedia*.

The concept for the Series came from discussion with Marjan Bace of Manning Publications Company. A gap exists between the way materials characterization is often presented and the needs of a large segment of the audience—the materials user, process engineer, manager, or student. In our experience, when, at the end of talks or courses on analytical techniques, a question is asked on how a particular material (or processing) characterization problem can be addressed the answer often is that the speaker is "an expert on the technique, not the materials aspects, and does not have experience with that particular situation." This Series is an attempt to bridge this gap by approaching characterization problems from the side of the materials user rather than from that of the analytical techniques expert.

We would like to thank Marjan Bace for putting forward the original concept, Shaun Wilson of Charles Evans and Associates and Yale Strausser of Surface Science Laboratories for help in further defining the Series, and the Editors of all the individual volumes for their efforts to produce practical, materials user based volumes.

C. R. Brundle *C. A. Evans, Jr.*

MASIMO 1054
Masimo v. Apple
IPR2023-00634

Preface

Most ceramics are ionically bonded compounds found in complex crystal structures that are strong, stiff, lightweight, hard, and corrosion-resistant. Typically, they maintain their properties to high temperatures. In a broad sense, a ceramic is any man-made, inorganic, nonmetallic, solid material. Glass, usually considered a subset of ceramics, is any solid that lacks crystalline order. Traditionally, ceramics have been considered polycrystalline, although most ceramists today do not accept that restriction. Also traditional is the idea that high temperatures are required for the synthesis or processing of ceramics and glasses; but that limitation is no longer valid—new materials such as aerogels and tin fluorophosphate glasses are synthesized at room temperature or at a few hundred degrees above ambient.

Raw materials for ceramic and glass manufacture traditionally are earthy, oxide materials that are mined in high volume at low cost and are subjected to relatively little processing. The products made from them are commodity items such as brick, tile, bottles, and windows. Modern technical or engineering ceramics are higher-value materials that have superior properties as a result of more sophisticated processing and tighter control over raw materials. These advanced ceramics are much more varied in composition than simple oxides and include, for example, carbides, nitrides, and borides. The development of ceramic composites that are heterogeneous on the micrometer or nanometer scale is a rapidly expanding area of materials science and engineering. The need for better control of final properties requires increased use of modern characterization techniques at all stages of ceramic synthesis and processing. This volume describes characterization techniques and how they can be used to obtain that greater control.

This book is written in a time of changing priorities in materials science and engineering. Responding to a perception that research results in the United States were not being reliably translated into marketable products, the U.S. National Academy of Sciences conducted an influential study—the results of which were reported in a widely read book, *Materials Science in the 1990s: Maintaining Competitiveness in the Age of Materials*, National Academy Press, Washington, D.C., 1989—that recommended increased emphasis on materials synthesis and processing. These recommendations include

- interactive research on new materials synthesis that is linked with characterization and analysis of the product
- basic research on synthetic solid-state inorganic chemistry to produce new compounds

MASIMO 1054
Masimo v. Apple
IPR2023-00634

- synthesis of ultra pure materials, for example, fibers with low oxygen or carbon impurity levels
- research on techniques for synthesis to net-shape; that is, learning how to do synthesis, processing, and forming in a single step
- research on methods for processing ceramic materials far from equilibrium
- research on processing artificially structured or, as they are sometimes called, functionally gradient materials.

Characterization of Ceramics addresses these concerns and recommendations in two ways. First, the book stresses advanced synthesis and processing. Second, the central theme of the book, the application of characterization techniques, is a specific recommendation of the NAS study. The 13 chapters of this volume present a broad overview of ceramics and glasses. Each of the topics provides enough information for the reader to make intelligent choices among the myriad available characterization and analysis techniques. Many of the chapters are organized as case studies taken from the authors' own research, which help to illustrate how different methods can be integrated to give a more complete picture of a given process or phenomenon.

The first part of the book deals with the techniques of ceramic synthesis. Increasingly, advanced ceramics are being produced from highly processed powders made by methods collectively known as chemical preparation. Some of the more promising routes to the production of advanced ceramic powders are sol–gel processing, precipitation from solution, gas-phase synthesis, and powder-surface modification. J. A. Voigt discusses recent trends in the use of near–room temperature solution techniques to make ceramic precursors. An example of this is the sol–gel method, in which organometallic reagents in solution are hydrolyzed and condensed to form an inorganic polymeric gel that, when dried and fired, gives the desired ceramic composition. These chemical methods can generate controlled-size distributions, extremely reactive precursors, unusually shaped particles, and gels. Solution methods permit the intimate mixing of components, easy dispersion of second phases, and surface modification of precursor particles. Liquid precursor solutions also can be used to make thin films by dipping or spinning; because of the high reactivity of the precursor particles, film consolidation occurs at moderate temperatures. The chapter by R. W. Schwartz on electronic ceramics shows how analytical methods such as NMR are used to guide the solution synthesis of electronic ceramic films such as PZT (lead zirconate–lead titanate). Voigt's chapter illustrates the importance of thorough characterization in the development of better synthesis methods.

Ceramic powders and films made by gas-phase techniques and their characterization are discussed by C. L. J. Adkins and D. E. Peebles. Ultrafine ceramic particles with enhanced surface reactivity, such as SiO_2, can be synthesized through nucleation or condensation reactions in gas-phase aerosols. Ceramic films and

MASIMO 1054
Masimo v. Apple
IPR2023-00634

coatings, such as diamond and diamond-like materials, are synthesized by a variety of vapor deposition techniques.

Ceramic processing methods are extremely diverse, with new ones being constantly developed. The technique with widest application is sintering bulk ceramics, in which a powder preform is typically converted to a dense, consolidated object through solid or liquid-phase diffusion. The driving force for diffusion is the lowering of the Gibb's energy by minimizing surface area and, possibly, by reaction to more stable products. K. G. Ewsuk discusses the essential features of bulk sintering and the analytical methods used to characterize the process. By contrast, T. J. Garino's chapter is concerned with the densification of ceramic thick films and the phenomena distinctive to them. For example, ceramic films usually are deposited on substrates, and differential shrinkage in drying or firing leads to stresses and possibly warping. Garino's discussion emphasizes characterization methods applicable to those ceramic films.

Much current ceramic processing research for both bulk materials and films is directed toward eliminating flaws, thereby increasing strength and fracture toughness. L. Neergaard's chapter on nondestructive evaluation shows how to detect flaws that are frequently generated in a ceramic despite the best of processing efforts.

Other types of ceramic processing discussed in this volume are inorganic glasses and glass-ceramics by R. K. Brow, ceramic composites by S. J. Glass, and ceramic joining by A. P. Tomsia. This selection of processing methods is not exhaustive, but is broad enough for most of the applicable characterization techniques to be presented. These three chapters share a common concern with interfaces and how to characterize their reactivities, compositions, and microstructures.

Because ceramics are brittle, they are susceptible to catastrophic failure under mechanical load. The useful strength of a ceramic is determined by the flaw population: stresses are concentrated at flaws, which cause cracks to propagate to failure. The critical property for ceramics in load-bearing uses is not the strength, but the fracture toughness—the resistance of the ceramic to crack propagation. The fracture surface of a ceramic bears the evidence of its failure. One must read the features in a fracture surface to understand the origin and path of the fracture. The case study by E. K. Beauchamp shows how much practical information can be obtained from ceramic fracture analysis.

The other two chapters are basic to much of ceramics. In ceramics, microstructure determines properties; the study of that relationship has been a main theme for decades. A. H. Carim's chapter illustrates the range of microscopic and microanalytic techniques used to determine the structures and composition of ceramic microstructures. Another foundation of ceramics is reactivity and phase behavior. Knowledge of these topics is basic to understanding all forms of thermal processing of ceramics. P. K. Gallagher's chapter on reactivity and thermal analysis is an authoritative account by one of the experts of the field.

Ronald E. Loehman

MASIMO 1054
Masimo v. Apple
IPR2023-00634

EXHIBIT NNN

MASIMO 1054
Masimo v. Apple
IPR2023-00634

Fritz Aldinger and Volker A. Weberruß

Advanced Ceramics and Future Materials

An Introduction to Structures, Properties, Technologies, Methods



WILEY-VCH Verlag GmbH & Co. KGaA

MASIMO 1054
Masimo v. Apple
IPR2023-00634

The Authors

Prof. Dr. Fritz Aldinger
Max-Planck-Institut für Metallforschung
and
Universität Stuttgart
Institut für Nichtmetallische-Anorganische Materialien
Heisenbergstr. 3
70569 Stuttgart
Germany

Dr. Volker A. Weberruß
Max-Planck-Institut für Metallforschung
Pulvermetallurgisches Laboratorium (PML)
Heisenbergstr. 1
70569 Stuttgart
and
V.A.W. Scientific Consultation
Im Lehenbach 18
73650 Winterbach
Germany

Cover

The cover image shows a brake disc with titanium bell.
The image was kindly supplied by
SGL Brakes GmbH
Werner-von-Siemens-Str. 18
86405 Meitingen, Germany.

All books published by Wiley-VCH are carefully produced. Nevertheless, authors, editors, and publisher do not warrant the information contained in these books, including this book, to be free of errors. Readers are advised to keep in mind that statements, data, illustrations, procedural details or other items may inadvertently be inaccurate.

Library of Congress Card No.:
applied for

British Library Cataloguing-in-Publication Data
A catalogue record for this book is available from the British Library.

Bibliographic information published by the Deutsche Nationalbibliothek
The Deutsche Nationalbibliothek lists this publication in the Deutsche Nationalbibliografie; detailed bibliographic data are available on the Internet at http://dnb.d-nb.de.

© 2010 WILEY-VCH GmbH & Co. KGaA, Weinheim

All rights reserved (including those of translation into other languages). No part of this book may be reproduced in any form - by photoprinting, microfilm, or any other means - nor transmitted or translated into a machine language without written permission from the publishers. Registered names, trademarks, etc. used in this book, even when not specifically marked as such, are not to be considered unprotected by law.

Printing and Binding betz-druck GmbH, Darmstadt
Cover Design Schulz Grafik-Design, Fußgönheim

Printed in the Federal Republic of Germany
Printed on acid-free paper

ISBN: 978-3-527-32157-5

MASIMO 1054
Masimo v. Apple
IPR2023-00634